Cancer Research

MiR-10b Downregulates the Stress-Induced Cell Surface Molecule MICB, a Critical Ligand for Cancer Cell Recognition by Natural Killer Cells

Pinchas Tsukerman, Noam Stern-Ginossar, Chamutal Gur, Ariella Glasner, Daphna Nachmani, Yoav Bauman, Rachel Yamin, Alon Vitenshtein, Noah Stanietsky, Tomer Bar-Mag, Dikla Lankry, and Ofer Mandelboim

Abstract

Natural killer cells (NK) are a component of innate immunity well known for their potent ability to kill virus-infected or neoplastically transformed cells following stimulation of the NK cell receptor NKG2D. One of the various ligands of NKG2D is MICB, a stress-induced ligand that has been found to be upregulated on the surface of tumor cells. However, there is little knowledge about how this upregulation may occur or how it may be selected against in tumors as a mechanism of immune escape. Here, we report that the metastasis-associated microRNA (metastamir) miR-10b directly binds to the 3′ untranslated region of MICB and downregulates its expression. Notably, antagonizing miR-10b action enhanced NKG2D-mediated killing of tumor cells *in vitro* and enhanced clearance of tumors *in vivo*. Conversely, overexpression of miR-10b downregulated MICB and impaired elimination of tumor cells. Together, our results define MICB as a novel immune target of miR-10b, implying a direct link between metastasis capability and immune escape from NK cells. *Cancer Res; 72(21); 5463–72. ©2012 AACR.*

Introduction

MiRNAs are short noncoding RNA molecules that usually repress gene expression, by binding to their target mRNAs [mainly in the 3′ untranslated region (UTR)] and either repress translation, or cause mRNA degradation (1, 2). The miRNAs' effect is moderate; nevertheless, these molecules are important gene regulators (3–5) and it is estimated that the activity of more than 50% of all cellular genes is controlled by miRNAs (5). MiRNAs can be either beneficial or detrimental to the developing tumors as they could serve either as tumor suppressors or as tumor initiators (6–10). MiRNAs are also involved in the metastatic process and the capacity of several miRNAs to initiate and to promote metastasis formation set the term "metastamir" (11–13). The most prominent metastamirs are: miR-10b, miR-21, miR-210, miR-373, and miR-520d (11–14). Among these miRNAs, miR-10b is probably the most famous one as it promotes both invasion and metastasis in various types of cancers by targeting multiple genes (15–18). Surprisingly, miR-10b is also expressed in the majority of normal tissues (19). Furthermore, it is significantly downregulated in the initial process of breast cancer initiation and is later upregulated in tumor metastases (20, 11). These observations suggest that miR-10b also functions under normal conditions; however, its role under these conditions is poorly understood.

Developing tumors are sensed by both innate and adaptive immune cells (21). Natural killer (NK) cells, which are part of the innate immune system, are known for their capacity to kill various tumor cells (22, 23). NK cell activity is controlled by a balance of signals derived from inhibitory and activating receptors (24, 25). One of the most powerful activating receptors expressed by NK cells (and also by subsets of T cells) is NKG2D (26, 27). This receptor recognizes stress-induced ligands that appear on the cell surface following various stresses, such as viral infection and cell transformation (28). The human stress-induced ligands include the major histocompatibility complex class I polypeptide–related sequences A and B (MICA and MICB, respectively) and the UL16-binding proteins (ULBP) 1–6 (28–30). Numerous mechanisms were developed by tumors and by viruses to escape NKG2D-mediated recognition, emphasizing the importance of this receptor (29, 31–35). For example, several distinct cellular and viral miRNAs were shown to target MICB, MICA, and ULBP3 to evade the NKG2D-mediated elimination (31–35).

The identification of miRNA targets is a difficult task. This difficulty arises because miRNAs are not fully matched with their target mRNAs and because the exact mechanisms controlling miRNA-mRNA interactions are not fully understood. Most algorithms that were so far developed to predict miRNA targets are very inaccurate with a false positive rate of about 65% (36).

Because several of the cellular MICB/A-targeting miRNAs are overexpressed in tumors (35) and as NKG2D plays an important role in tumor cell recognition, we wondered whether tumors might use metastamirs not only to promote the

Authors' Affiliation: Lautenberg Center for General and Tumor Immunology, The Hebrew University, The BioMedical Research Institute, Hadassah Medical School, Jerusalem, Israel

Note: Supplementary data for this article are available at Cancer Research Online (http://cancerres.aacrjournals.org/).

Corresponding Author: Ofer Mandelboim, The Hebrew University, Ein Karem, Jerusalem, MA 91120, Israel. Phone: 972-2-6757515; Fax: 972-2-6424653; E-mail: oferm@ekmd.huji.ac.il.

doi: 10.1158/0008-5472.CAN-11-2671

generation of the metastatic phenotype but also to facilitate evasion from immune detection, by targeting the stress-induced ligands of NKG2D. Here, we show that MICB is targeted by the metastamir miR-10b and that such targeting leads to tumor escape from NK cell attack.

Materials and Methods

Lentiviral constructs, production, and transduction

Artificial RNA hairpins that function as pre-miRNA hairpins were generated by using the pTER vector as previously described (37). Sponge constructs were generated by annealing the oligonucleotides, phosphorylating them using T4 polynucleotide kinase, and inserting them into the pcDNA3 vector (Invitrogen). The sponges were excised and cloned into the lentiviral vector SIN18-pRLL-hEFIap EGFP-WRPE (38), downstream to the GFP cassette. Each sponge consists of 6 adjacent binding sites for the relevant viral miRNA, separated by a 4 nucleotide (AGAG) spacer (Hannon 2008). The sequences of the sponges binding site: sponge anti–hsa-miR-10b: (5′–3′) CACAAATTCGGAAGACAGGGTA; Sponge anti–miR-BART 1-5p (control): CACAGCACGTCAGAACACTAAGA. The MICB coding sequence was inserted into the SIN18-pRLL-hEFIap EGFP-WRPE instead of the GFP as previously described (35). Lentiviral vectors were produced as previously described (35).

Cytotoxicity assays and NK cell preparation

The cytotoxic activity of NK cells against various targets was assessed for 5 hours in ^{35}S methionine release assays as described (39). The final concentration of the blocking antibodies was 2.5 mg/mL. NK cells were isolated from peripheral blood using the human NK cell isolation kit and the autoMACS instrument (Miltenyi Biotec) according to the manufacturer's instructions.

Cell lines and antibodies

The following cell lines were used: HeLa (ATCC number CCL-2), PC-3 (ATCC number CRL-1435), DU 145 (ATCC number HTB-81), HEK 293T (ATCC number CRL112-68), RKO (ATCC number CRL-2577), MDA-MB-231 (ATCC number HTB-26), and MCF7 (ATCC number HTB-22). All cell lines in this work were obtained from and validated by the American Type Culture Collection and maintained as per instructions. The anti-MICA, anti-MICB (MAB1599; no cross-reaction with any of the stress ligands), anti–ULBP1-3, and anti-NKG2D antibodies were all purchased from R&D Systems. The anti-CD99 (12E7) was used as an isotype control. The anti-NKG2D hybridoma C7 used for the *in vivo* NKG2D blocking was kindly provided by Profs. M.W. Yokoyama (Washington University, St. Louis, MO) and S. Jonjic (University of Rijeka, Rijeka, Croatia). The anti-NK1.1 (PK136) was used for NK cells depletion.

Real-time PCR

Total RNA was isolated from various cell lines by using the Tri-Reagent (Sigma) and treated with RNase-free DNase-Turbo (Ambion). The RNA extraction and cDNA preparation were done as previously described (34). MiR-16 and U6 snRNA were used as the endogenous reference genes for PCR quantification. The reverse primer was a 3′ adapter primer (3′RACE outer primer in the First Choice RLM-RACE Kit), and the forward primer was designed based on the entire miRNA sequence. For hsa-miR-10b: 5′- TACCCTGTAGAACCGAATTTGTG 3′. The relative expression was calculated by qbase algorithm when lowest expression was set to 1 in the miRNAs. The MICB mRNA levels were quantified using MICB specific Taqman Gene Expression Kit by Ambion according to the manufacturer's instructions. hypoxanthine phosphoribosyltransferase was used as a control gene.

DNA constructs and luciferase assay

For the firefly luciferase vector, we used the pGL3 control vector (Promega). The 3′UTR of MICB was generated as described (35) Xba I site immediately downstream to a stop codon. The inserts and their proper orientation were confirmed by sequencing. The mutation in has-miR-10b was generated using following primers: FW 5′ TTCAGTCCAATACACCGTTGTGGG REV 5′ CCCACAACGGTGTATTGGACTGAA, the luciferase assay was conducted as described (32).

Lung clearance assay

Male C57B/6 mice (9–10 weeks old) were divided into 3 groups and were injected IP with anti-mouse NKG2D mAb (C7) at a concentration of 300 μg per mouse, or with NK1.1 (PK136), 150 μg per mouse or PBS. Twenty-four hours later, HeLa cells [cells that are not efficiently killed by mouse NK cells (40), thus serving as internal control] were labeled with the fluorescent dye Vybrant DiD (Molecular Probes) and the various PC-3 cells were labeled with the fluorescent dye CFSE (Molecular Probes). Cells were mixed at a density of 5×10^6 cells of each population in 1 mL of PBS, and 400 μL was injected into the tail vein. Lungs were collected 5 hours later, single-cell suspensions were obtained with cell strainers, and fluorescence was analyzed by fluorescence-activated cell sorting (FACS). The ratio of tested target cells to HeLa cells was calculated. The ratio of the control vector injected cells to HeLa was set as 100%.

Results

MiR-10b specifically downregulates MICB expression

To investigate whether metasamirs are involved in immune regulation by targeting the stress-induced ligands of NKG2D, we used the TargetScan algorithm (41) and searched the 3′ UTRs of the stress-induced ligands of NKG2D for potential binding sites of prominent metastasis-prompting miRNAs, miR-10b, miR-21, and miR-210. Potential binding sites were predicted in the 3′ UTRs of MICB, ULBP1, and ULBP2 (Supplementary Fig. 1) with regard only to miR-10b, thus we continued our analysis with this miRNA.

MiR-10b and a control miRNA were cloned into lentiviral vectors that also contain a GFP cassette and the 2 miRNAs were transduced into RKO cells (the transduction efficiencies of all cell lines used in this article are shown in Supplementary Fig. 2). As can be seen in Fig. 1A and quantified in Fig. 1B, expression of miR-10b, resulted in about 50% downregulation of MICB expression compared with cells transduced with a control miRNA.

It has previously been shown that the expression of miR-10b differs substantially between the 2 breast cancer lines,

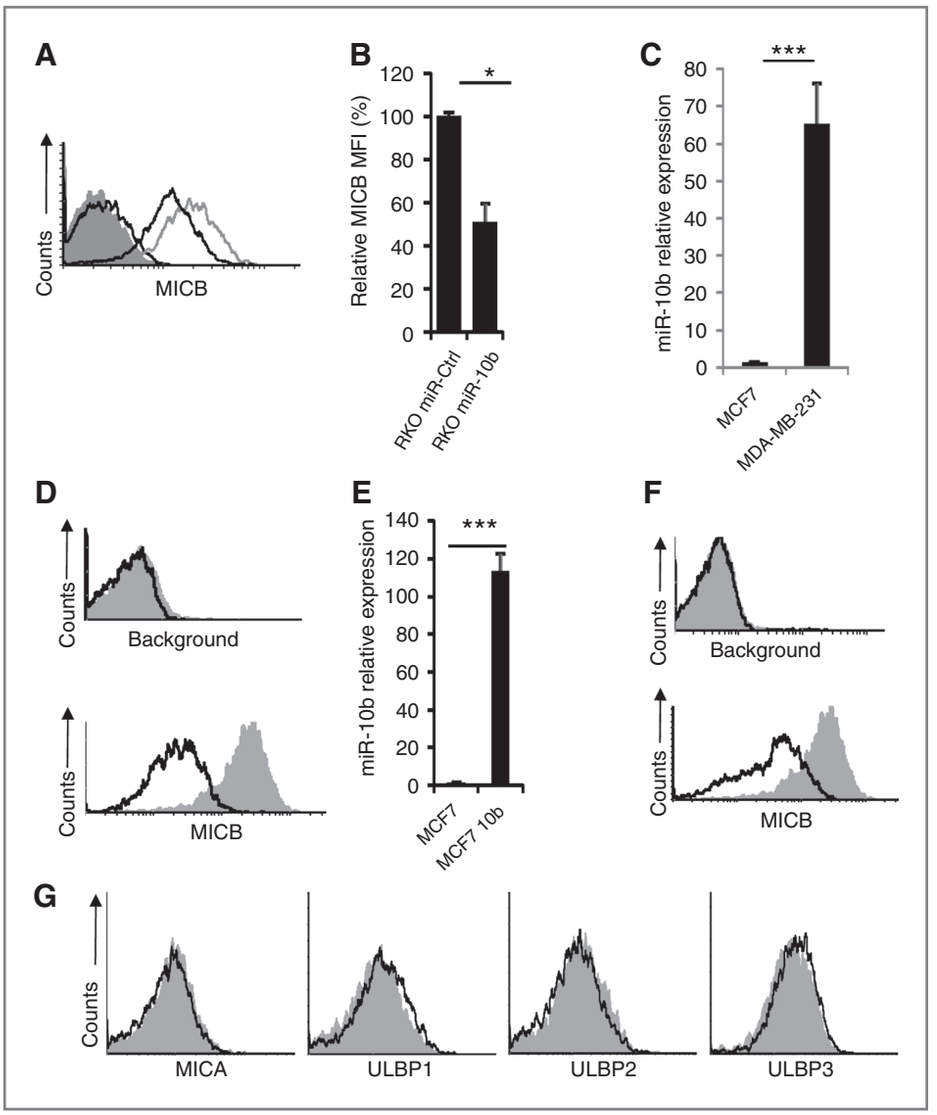

Figure 1. MiR-10b specifically downregulates MICB expression. A, FACS analysis of MICB expression in RKO cells transduced with miR-10b (black open histogram) or with a control miR-BART 1-5p (gray open histogram). The filled gray histogram represents the staining of the secondary mAb only. The black open histogram that overlays the control filled gray histogram is the background staining of the control miRNA. B, quantification of the miR-10b effect. The MFI of MICB in the Ctrl miR–transduced cells was set up to be 100% and the decrease in the miR-10b–transduced cells was calculated accordingly. *, $P < 0.03$ by 2-tailed Student *t* test. C, the relative expression levels of miR-10b in the cell lines indicated in the *x*-axis. ***, $P < 0.0006$ by 2-tailed Student *t* test. D, top histograms represent background staining. Bottom histograms show MICB expression in MDA-MB-231 (black open histogram), compared with the expression of MICB in MCF7 cells (gray filled histogram). E, the relative levels of miR-10b expression in MCF7 cells following miR-10b transduction (the parental MCF7 levels of miR-10b set as one). ***, $P < 0.0003$ by 2-tailed Student *t* test. F, top histograms show background staining; bottom histograms show MICB expression in MCF7 cells overexpressing miR-10b (black open histogram) compared with the parental MCF7 cells (gray filled histogram). G, FACS analysis of the expression of NKG2D ligands (other than MICB, only ligands that are expressed by MCF7 cells are shown), by MCF7 cells. Cells overexpressing miR-10b are indicated by the black open histogram, and stress ligands other than MICB expressed by MCF7 cells overexpressing the control miR-BART 1-5p are indicated by the gray filled histogram. The background staining of MCF7 cells presented in G is shown in F, top. The entire figure shows one representative experiment out of 3 conducted.

MDA-MB-231 and MCF7 (11). After confirming these observations (Fig. 1C), the expression of miR-10b in MCF7 cells was set up as one. We have tested the surface expression levels of MICB in these 2 cell lines and observed that, in agreement with the above results, MICB levels were inversely correlated with the expression of miR-10b (Fig. 1D). We next overexpressed miR-10b in MCF7 cells (Supplementary Figs. 2 and 1E) and observed that this overexpression significantly reduced MICB expression (Fig. 1F). Although the TargetScan algorithm predicted that ULBP1 and ULPB2 can potentially be targeted by miR-10b (Supplementary Fig. 1), little, or no changes in the levels of these ligands or other NKG2D ligands was detected in the presence of miR-10b (Fig. 1G, figure shows only the stress-induced ligands that are expressed by this cell line). Therefore, we concluded that miR-10b specifically controls MICB expression.

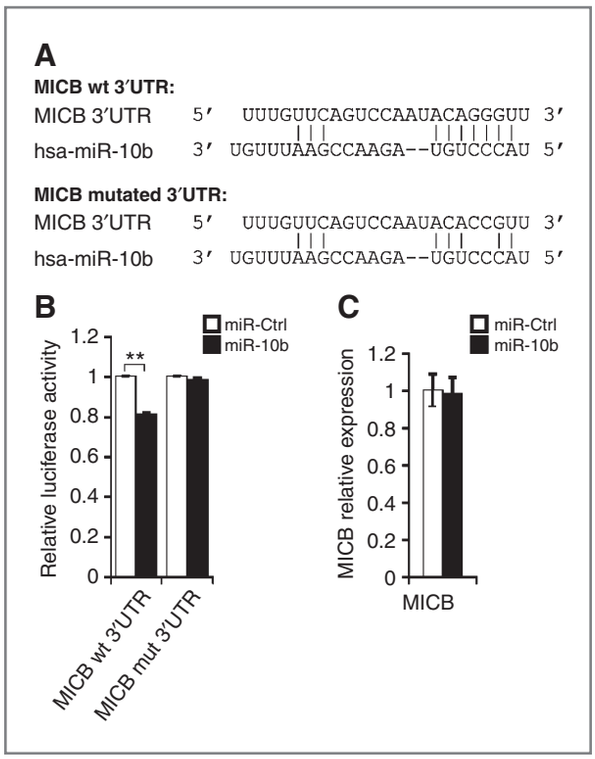

Figure 2. MiR-10b directly binds the 3′UTR of MICB. A, upper, schematic representation of the 3′ UTR of MICB and the predicted binding of miR-10b (seed position bases 570–576 in the 3′UTR of MICB). Lower, alignment of miR-10b and the mutated 3′UTR of MICB. B, relative luciferase activity after transfection of the indicated reporter plasmids; MICB 3′UTR or the mutant MICB mut-10b 3′UTR (indicated in the *x*-axis) into RKO cells expressing either hsa-miR-10b (black) or the control miR BART 1-5p (miR-Ctr, white). Firefly luciferase activity was normalized to Renilla luciferase activity and then normalized to the average activity of the control reporter. Shown are mean values ± SD. Statistically significant differences are indicated. **, $P < 0.02$ by 2-tailed Student *t* test. Error bars (SD) are derived from triplicates. Figure shows 1 representative experiment of 3 conducted. C, levels of MICB mRNA were measured by qRT-PCR in RKO cells overexpressing miR-10b (black) or control miR-BART-4 (white). Results are representative of 3 independent experiments.

MiR-10b directly binds to the 3′ UTR of MICB

To test whether miR-10b targets MICB directly we generated 2 firefly luciferase constructs; one containing the wild-type 3′UTR of MICB and another one containing the 3′UTR of MICB, in which the miR-10b site [predicted by the TargetScan algorithm (Fig. 2A)] was mutated. These constructs were transiently transfected into RKO cells that were also transduced with miR-10b, or with a control miRNA. As can be seen in Fig. 2B, a moderate, yet significant decrease in luciferase activity was observed in the presence of miR-10b, whereas the mutations in the 3′UTR of MICB abolished this effect, indicating that miR-10b indeed directly targets MICB at the predicted binding site.

To elucidate the mechanism accounting for the miR-10b–mediated downregulation of MICB we used quantitative real-time PCR (qRT-PCR) to evaluate the mRNA levels of MICB in RKO cells stably expressing miR-10b or a control miRNA. In agreement with our previous reports about the miRNA mode of regulation of the stress-induced ligands (34, 35), we observed no significant differences (Fig. 2C), suggesting that the miR-10b–mediated MICB downregulation probably occurs by translational repression.

Subtle changes in MICB expression affects NKG2D-mediated killing

The miRNA activity effect is generally moderate (3) and indeed the miR-10b–mediated downregulation of MICB was moderate as well, ranging between 20% and 50% depending on the cell line examined (see Fig. 1 and figures below). We were, therefore, interested to test whether moderate differences in MICB expression will affect the NKG2D-mediated killing by NK cells. For this purpose, we transduced 293T cells (that do not express MICB on their cell surface) with lenti viruses expressing MICB and obtained 3 clones expressing various levels of MICB on their surface (Fig. 3A). The various MICB-expressing clones were then used in NK cytotoxicity assays. As can be seen in Fig. 3B and C subtle changes of around 20% of MICB expression were sufficient to cause a significant reduction in the NK-mediated killing of 293T cells (the raw killing data are presented in Supplementary Fig. 3). The MICB-dependent reduction of killing was due to reduced NKG2D recognition, because the killing of all clones was reduced to the levels of the parental 293T upon NKG2D blocking (Supplementary Fig. 3).

The downregulation of MICB by miR-10b results in reduced NKG2D-mediated killing

We next aimed to show that the miR-10b–mediated downregulation of MICB is functional and specific. We, therefore, initially tested whether the expression of miR-10b in a cell line deficient for MICB expression such as 293T (Supplementary Fig. 4) will alter either the expression of the NKG2D ligands or will affect the killing of these cells. As can be seen, overexpression of miR-10b did not induce the expression of MICB and it did not influence the expression of other NKG2D ligands such as MICA, ULBP2, and ULBP3 (Supplementary Fig. 4A). Furthermore, no difference in the killing of 293T cells was observed between miR-10b–transduced and control miR–transduced cells (Supplementary Fig. 4B).

Next, we tested the functional outcome of the miR-10b targeting of MICB by using various cell lines of diverse origins that are positive for MICB expression such as: DU 145 cells (Fig. 4A), MCF7 (Fig. 4B), and RKO (Fig. 4C). The cells were transduced with miR-10b or with a control miR (the transduction efficiency is shown in Supplementary Fig. 2) and as can be seen in Fig. 4A–C, column 1, quantified in Fig. 4A–C, column 2, a reduction in MICB expression was noticed in all cell lines following the miR-10b overexpression. Furthermore, the miR-10b–mediated reduction was specific as the expression of other NKG2D ligands was not altered following the miR-10b transduction (Fig. 1G and Supplementary Fig. 5, figure shows only the NKG2D ligands that are expressed by these cells).

Next, we tested whether the miR-10b–mediated reduction of MICB expression is functional. For that we used all cell lines transduced with miR-10b in NK cytotoxicity assays. As can be

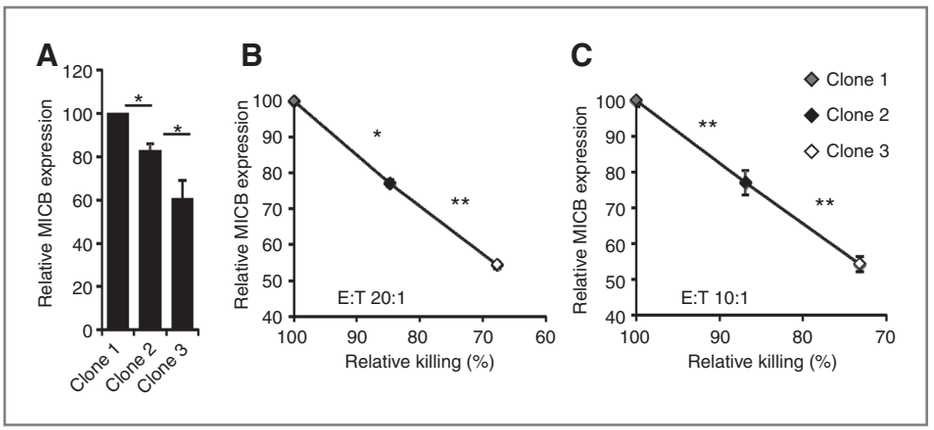

Figure 3. Moderate changes in MICB levels affect NK cell cytotoxicity. A, relative MICB expression levels in the various 293T transfectants. The clone expressing the highest median fluorescence intensity of MICB expression was set up to be 100%. The differences are statistically significant; *, $P < 0.05$ by 2-tailed Student *t* test. B and C, NK killing is significantly affected by MICB levels. Bulk NK cells were incubated with the various 293T clones shown in A for 5 hours at E:T (effector to target) ratio 20:1 (B) or 10:1 (C). The 293T cell clone expressing the highest MICB expression levels is indicated by gray-filled rhombus. Intermediate expression is indicated by black rhombus, and the lowest MICB expression is indicated by empty rhombus. *, $P < 0.05$ by 2-tailed Student *t* test; **, $P < 0.02$ by 2-tailed Student *t* test. *Y*-axis represents relative MICB expression levels (%), *x*-axis normalized killing. The raw data, the NKG2D-blocking experiments, and the killing of the untransduced 293T cells are presented in Supplementary Fig. 3. Results are representative of 3 independent experiments.

seen in Fig. 4A–C, column 3, the miR-10b–mediated reduction of MICB expression is functional as it leads to a moderate reduction in killing of all 3 target cells tested at various effector to target ratios. Furthermore, the miR-10b–mediated reduction of killing was caused by reduced NKG2D recognition as blocking of NKG2D resulted in equivalent killing of all targets (Fig. 4C, column 3). Thus, we concluded that targeting of MICB by miR-10b leads to a specific reduction of MICB expression and consequently to reduced killing by NK cells.

MiR-10b endogenously controls MICB expression

We next wanted to show that MICB expression is endogenously controlled by miR-10b. For this purpose, we used the miRNA sponge technique that enables us to antagonize the activity of a certain miRNA (42). HeLa cells and PC-3 cells that express moderate levels of miR-10b and DU 145 cells that express high levels of miR-10b were transduced with either the anti–miR-10b sponge, or with a control sponge (the transduction efficiency is shown in Supplementary Fig. 2). As can be seen in Fig. 5A–C, column 1, quantified in 5A–C, column 2 the expression of the miR-10b sponge leads to a moderate elevation of about 25% in MICB expression. The increased expression of MICB was specific and significant as the expression of other NKG2D ligands did not change (Supplementary Fig. 6, the figure show only the staining of NKG2D ligands that are expressed by these cells). The sponge effect is moderate because the sponge does not completely prevent the MICB targeting by the relevant miRNA, but it rather titrates some of the miRNA effect through target site competition (42).

One of the major advantages of the sponge technique is that it also enabled us to monitor for the sponge activity. The sponge is located downstream to the GFP open reading frame and thus the sequestration of the relevant miRNA leads to reduced GFP intensity. Indeed, as can be seen in Fig. 5A–C, column 3, the anti–miR-10b sponge indeed sequestered miR-10b as the GFP intensity of this sponge was significantly reduced in all lines tested as compared with control sponge.

Finally, we showed that the miR-10b–mediated sponge elevation of MICB expression is functional, as killing of the miR-10b sponge–transduced cells was enhanced in all lines tested (Fig. 5A–C-4). The increased effect was NKG2D dependent as blocking of NKG2D abolished the observed differences (Fig. 5C-4).

MiR-10b–mediated immune evasion *in vivo*

Our next aim was to show the significance of the miR-10b targeting of MICB *in vivo*. This is a difficult task because the human NKG2D ligands are different from those of the mouse and MICB is not expressed by mouse cells (43, 44). Furthermore, the 3′ UTRs of the mouse and human NKG2D ligands are different and no sites are predicted for miR-10b in the 3′UTRs of the mouse NKG2D ligands. Indeed, overexpression of miR-10b in the mouse B12 cells did not decrease the levels of mouse stress-induced ligands (data not shown). In addition, it is very difficult to examine the immune mediated effect of miR-10b in long-term assays using human xenograft implanted in T-cell–deficient mice, as miR-10b is very well known for its tumorogenic and metastatic properties. Thus, it would be very difficult to interpret the results that relate to the immune activity of miR-10b using long-term human xenograft assays.

On the other hand, testing the activity of NKG2D-related functions on human tumors is feasible in immunocompetent mice model as the murine NKG2D receptor recognizes the human ligands and vice versa (35). Thus, to evaluate the miR-10b–mediated immune effect *in vivo* we used a short term *in vivo* assay (illustrated in Fig. 6A). C57B/6 mice were injected either with PBS, with a blocking anti-NKG2D mAb [which does not lead to immune cell depletion (45)], or with anti-NK1.1 antibody for the depletion of NK cells, at time point zero (Fig. 6A). Twenty-four hours later, the various mice were intravenously (i.v.) injected with either PC-3 cells expressing

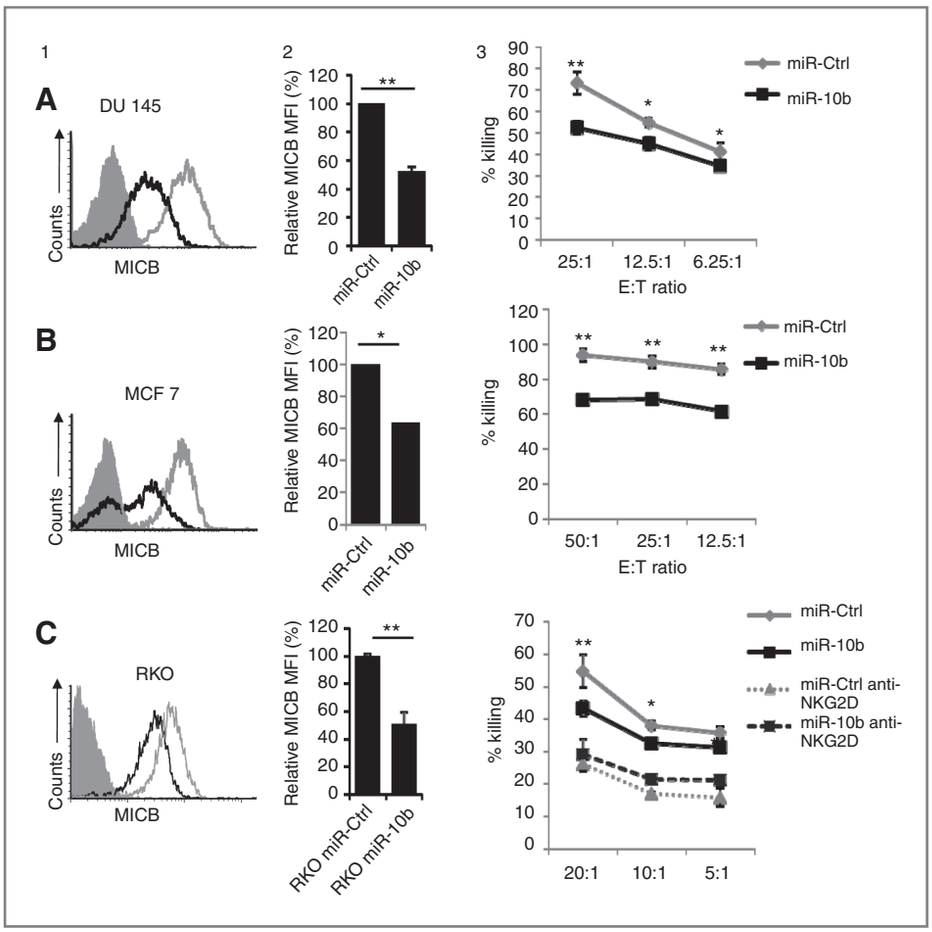

Figure 4. The miR-10b–mediated downregulation of MICB resulted in decreased NKG2D-mediated cytotoxicity. For clarity, we designated each row with a letter and each column with a number. Each row represents experiments conducted on the same cell line: DU 145 (A), MCF7 (B), and RKO (C). Column 1 shows FACS staining; column 2, quantification of the FACS staining; and column 3 shows NK killing assays. A to C, column 1, FACS analysis of MICB expression in cells transduced with miR-10b (black open histogram) or with a control miR-BART 1-5p (gray open histogram). The filled gray histogram represents the staining of the secondary mAb only. A to C, column 2, quantification of the miR-10b effect. The MFI of MICB in the Ctrl miR–transduced cells was set up to be 100% and the decrease in the miR-10b–transduced cells was calculated accordingly. *, $P < 0.03$; **, $P < 0.01$ by 2-tailed Student *t* test. A to C, column 3, cytotoxicity assays. Bulk NK cells were incubated with the indicated ^{35}S methionine-labeled cells expressing either miR-10b, or control miR-BART 1-5p (Ctrl miR) for 5 hours at the E:T ratios indicated at the *x*-axis. Shown are mean values ± SD. Statistically significant differences are indicated (*, $P < 0.05$; **, $P < 0.02$ by 2-tailed Student *t* test). C, column 3, in RKO cells, blocking experiments were also conducted in which an anti–NKG2D-blocking mAb (dashed lines) was included in the assays. The entire figure shows one representative experiment out of 3 conducted.

miR-10b (the specific downregulation of MICB is shown in Fig. 6B and Supplementary Fig. 7), PC-3 cells expressing a control vector, or PC-3 expressing an anti–miR-10b sponge (the specific upregulation of MICB is shown in Fig. 6B and Supplementary Fig. 7). As i.v. injections might vary between the different mice, it is essential to use an internal control. Therefore, in each injection, we mixed the tested PC-3 cells, which were labeled with one fluorescent dye, together with HeLa cells that were hardly killed by mouse NK cells (40) and that were labeled with a different fluorescent dye, and injected them i.v. into the various mice groups (Fig. 6A). The labeled cells reached the lungs of the injected mice within less than 1 minute (ref. 40 and Supplementary Fig. 8A) and the *in vivo* killing of the various cells was conducted in the lungs. The lungs of the injected mice were harvested 5 hours later, enabling us to examine the function of mainly innate immune cells, such as NK cells. Cell suspensions from the lungs were obtained and analyzed by FACS.

Importantly, we observed that the miR-10b–mediated downregulation of MICB was significant in this *in vivo* setting because, as can be seen in Fig. 6C, left, significantly more PC-3 cells overexpressing miR-10b were present in the lungs of the injected mice as compared with PC-3 cells expressing a control miRNA (miR-10b downregulates MICB, therefore, less cells are killed and more cells are present in the lungs). A reciprocal picture was observed when the miR-10b activity was antagonized by the miR-10b sponge as this led to a significantly lower tumor cell survival in the lungs (the miR-10b sponge leads to increased MICB expression and, therefore, increased killing). The differences observed were due to NKG2D recognition as the *in vivo* blocking of NKG2D activity by anti-NKG2D mAb abolished the effects observed (Fig. 6C, middle). Furthermore,

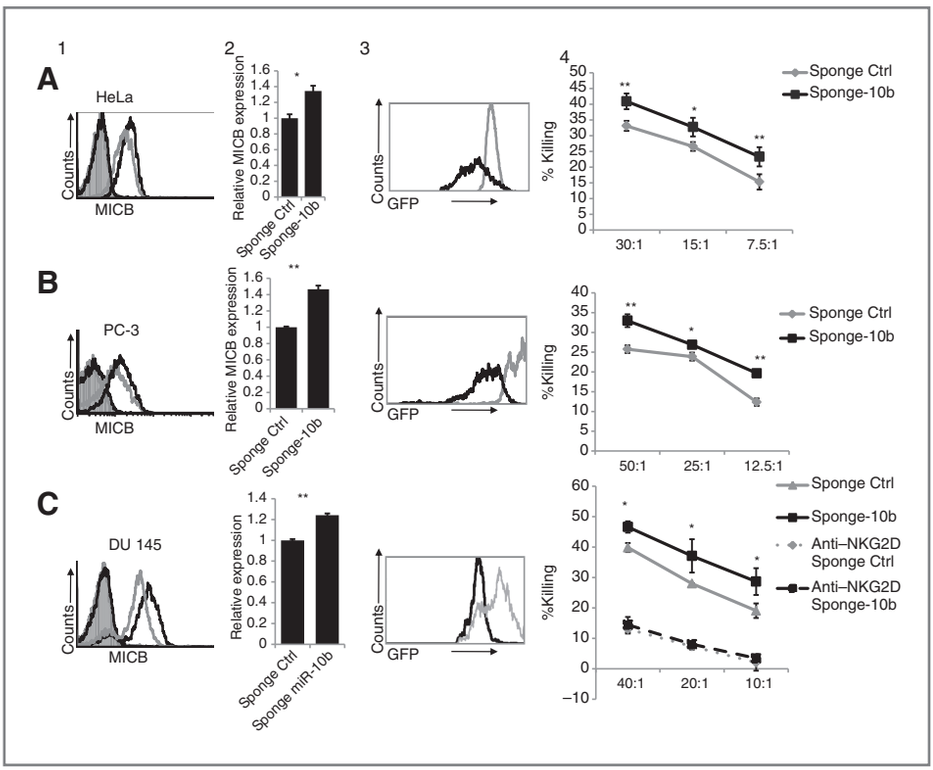

Figure 5. Endogenous control of MICB expression by miR-10b. For clarity, we designated each row with a letter and each column with a number. Each row represents experiments conducted on the same cell line: HeLa (A), PC-3 (B), and DU 145 (C). Column 1 shows FACS staining; column 2, quantification of the FACS staining; column 3, FACS of GFP intensity; and column 4, NK killing assays. A to C, column 1, FACS analysis of MICB expression in cells transduced with sponge-10b (black open histogram), or with a control sponge BART 1-5p (gray open histogram). The filled gray histogram represents the staining of the secondary antibody only. The black open histogram that overlays the control filled gray histogram is the background staining of the control miRNA. A to C, column 2, quantification of the sponge-10b effect. The MFI of MICB in the Ctrl miR–transduced cells was set up to be 1, and the increase in the MICB expression in the sponge-10b–transduced cells was calculated accordingly. *, $P < 0.03$; **, $P < 0.01$ by 2-tailed Student t test. A to C, column 3, the effect on GFP levels following miR-10b sequestration. The GFP levels in the sponge miR-10b–transduced cells are indicated by empty black histogram. The GFP levels in the control sponge–transduced cells are indicated by empty gray histogram. A to C, column 4, bulk NK cells were incubated with the indicated ^{35}S methionine-labeled cells expressing either sponge-10b or control sponge-BART 1-5p (Sponge Ctrl) for 5 hours at the effectors:target (E:T) ratios indicated at the x-axis. Shown are mean values $\pm$ SD. Statistically significant differences are indicated (*, $P < 0.05$; **, $P < 0.02$ by 2-tailed Student t test). C, column 4, in DU 145 cells, blocking experiments were also conducted in which an anti–NKG2D-blocking mAb (dashed lines) was included in the assay. The entire figure shows 1 representative experiment of 3 conducted.

NK cells are the main responders in this setting as the experiments were conducted for 5 hours only (enabling the activity of mainly innate immune cells) and because the depletion of NK cells by the anti-NK1.1 mAb completely abolished the effects observed (Fig. 6C, right). Examples of the raw data are presented in Supplementary Fig. 8. Thus, the miR-10b–mediated reduction of MICB protects tumor cells from immune recognition *in vivo*.

Discussion

Tumors have developed various mechanisms to escape immune cell–mediated elimination (21). Prominent among these, is the reduction of MHC class I expression to avoid CTL attack (46). However, evading CTL attack in such a manner renders the tumor cells susceptible to NK cell–mediated eradication, because NK cell killing is inhibited by MHC class I–binding inhibitory receptors (25, 44). To overcome the NK cell attack, tumors also developed mechanisms to inhibit the NK cell activity, which includes, for example, the upregulation of HLA-G to inhibit NK cytotoxicity (46), and the downregulation of killer ligands for NKG2D and NKp46 (35, 44, 47) to escape the killer receptor recognition.

In recent years, it was realized that several miRNAs contribute significantly to tumor spread and metastasis, hence these miRNAs were named oncomirs or metastamirs. Here, we identified a novel immune target for one of the most prominent metastamirs known to date, miR-10b. We show *in vitro* that miR-10b targets the 3′ UTR of MICB and not other stress-induced ligands and that this results in diminished NKG2D recognition and consequently reduced tumor cell killing by NK cells. We showed that the miR-10b–mediated downregulation of MICB resulted in reduced NK cell elimination *in vivo* through reduced recognition of NKG2D. This was a challenging task as MICB is not expressed in mice, the murine stress ligands are not targeted by miR-10b and it is quite difficult to assess the immune function of miR-10b as this miRNA is very well known for its prominent role in promoting tumor progression and metastases.

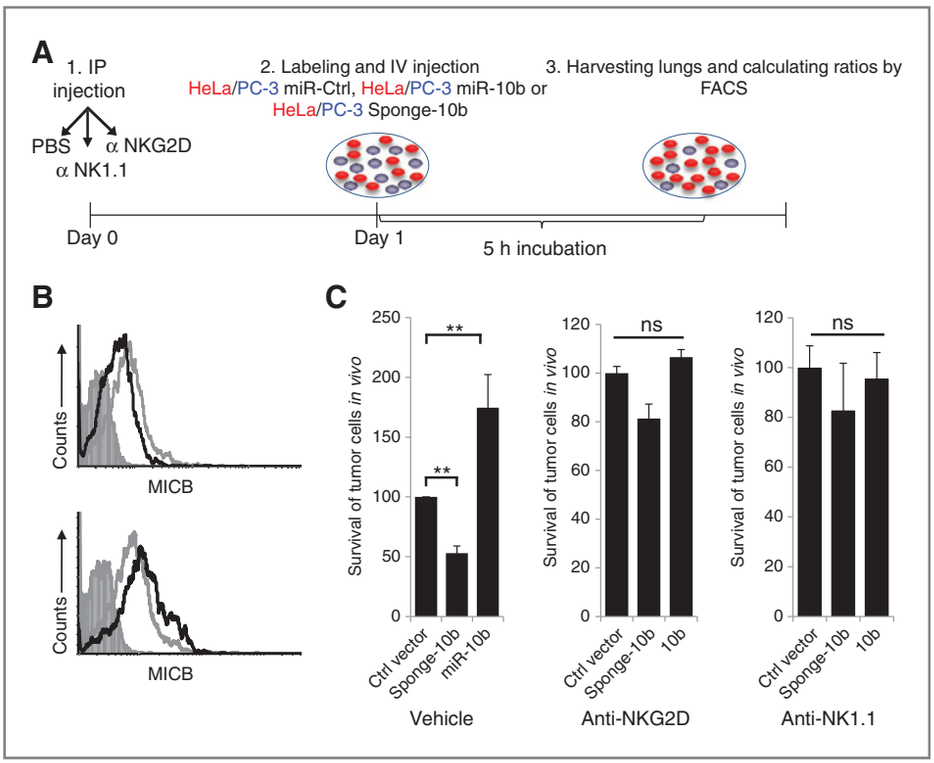

Figure 6. *In vivo* experiments. A, schematic representation of the *in vivo* experimental procedure (1). C57B/6 mice were injected intraperitoneally (IP) with anti-mouse NKG2D mAb, anti-NK1.1, or PBS (day 0; 2). Twenty-four hours later (day 1), labeled HeLa cells (used as internal control) were mixed at 1:1 ratio with labeled PC-3 cells overexpressing miR-10b, PC-3 cells expressing sponge-10b, or PC-3 cells expressing a control vector and injected i.v. into the C57B/6 mice (3). Five hours later, lungs were harvested and FACS analysis was done. B, FACS analysis for the expression of MICB on PC-3 cells. B, top, miR-10b overexpression is indicated by the black empty line, the control miR is indicated by gray empty line, and the filled gray histogram represents the staining of the secondary antibody only. Bottom, the sponge against miR-10b is indicated by the black empty line, the control sponge is indicated by gray empty line, and the filled gray histogram represents the staining of the secondary antibody only. C, left, PC-3 to HeLa ratio of tumor cells that are present in the lungs was calculated 5 hours postinjection, relative to the ratio of PC-3 to HeLa cells inoculated. The ratio of control vector PC-3 to HeLa cells was set up to be 100%. PC-3–expressing sponge-10b and PC-3 cells expressing miR-10b were calculated accordingly. **, $P < 0.01$, by 2-tailed *t* test. C, middle and right, the various mixtures of PC-3 and HeLa cells that were used in C, left, were injected into mice that were pretreated either with anti–NKG2D-blocking mAb (C, middle) or with anti-NK1.1 mAb (C, left). Tumor cell survival was calculated as in C left. Figure shows 1 representative experiment of 2.

We have previously identified other cellular miRNAs that target MICB (32, 35). The various MICB-targeting miRNAs share several features: First, all cellular MICB-targeting miRNAs inhibit its expression probably through inhibition of translation. Second, cells expressing each of the MICB-targeting miRNAs are killed less efficiently. Still, among the various MICB-targeting miRNAs, miR-10b seems to be a unique miRNA. Its binding site is located in the middle of the 3′ UTR of MICB and not at the edges as all other MICB-targeting miRNAs (32, 35). Furthermore, for all other MICB-targeting cellular miRNAs, viral miRNAs were identified that bind MICB in sites overlapping with the cellular miRNA-binding sites (32, 35). In contrast, no viral miRNAs were identified that target MICB at sites overlapping with that of miR-10b. Recent work by the Weinberg group showed that antagonizing miR-10b activity *in vivo* restores the levels of the transcription factor HOXD10 and reduces metastases formation (48, 49). Here, we show that a competitive inhibitor (sponge) directed against miR-10b led to the upregulation of MICB on the surface of tumor cells, resulting in significant clearance of tumor cells *in vivo*. Thus, we suggest that antagonizing miR-10b activity during tumor development may lead to reduction of metastases formation through dual mechanism by enhancing the expression of the transcription factor HOXD10 and by boosting the NKG2D-mediated immune attack.

In conclusion, we show here that the metastamir miR-10b targets MICB to avoid the NKG2D-mediated immune attack. NKG2D is expressed not only by NK cells but also by by CD8+ T cells where it functions as costimulatory molecule (50). Thus, targeting of MICB by miR-10b is a novel and general immune evasion mechanism that links directly metastases formation and immune evasion.

Disclosure of Potential Conflicts of Interest

No potential conflicts of interest were disclosed.

Authors' Contributions

Conception and design: P. Tsukerman, N. Stern-Ginossar, O. Mandelboim
Development of methodology: P. Tsukerman, D. Nachmani, D. Lankry, O. Mandelboim

Acquisition of data (provided animals, acquired and managed patients, provided facilities, etc.): A. Glasner, Y. Bauman, N. Stanietsky, T. Bar-Mag, D. Lankry
Analysis and interpretation of data (e.g., statistical analysis, biostatistics, computational analysis): P. Tsukerman, A. Vitenshtein, O. Mandelboim
Writing, review, and/or revision of the manuscript: P. Tsukerman, Y. Bauman, R. Yamin, A. Vitenshtein, N. Stanietsky, O. Mandelboim
Administrative, technical, or material support (i.e., reporting or organizing data, constructing databases): C. Gur, D. Lankry
Study supervision: O. Mandelboim

Acknowledgments

The authors thank Mazal Elnekave for assistance in the *in vivo* experiments.

Grant Support

This study was supported by grants from the Israeli Science Foundation, The ICRF, by the Rosetrees trust, by the Association for International Cancer Research (AICR), and by the I-CORE Program of the Planning and Budgeting Committee, The Israel Science Foundation (grant number 41/11). O. Mandelboim is a Crown professor of Molecular Immunology.

The costs of publication of this article were defrayed in part by the payment of page charges. This article must therefore be hereby marked *advertisement* in accordance with 18 U.S.C. Section 1734 solely to indicate this fact.

Received August 8, 2011; revised July 5, 2012; accepted August 6, 2012; published OnlineFirst August 21, 2012.

References

1. Guo H, Ingolia NT, Weissman JS, Bartel DP. Mammalian microRNAs predominantly act to decrease target mRNA levels. Nature 2010;466:835–40.
2. Jing Q, Huang S, Guth S, Zarubin T, Motoyama A, Chen J, et al. Involvement of microRNA in AU-rich element-mediated mRNA instability. Cell 2005;120:623–34.
3. Bartel DP. MicroRNAs: genomics, biogenesis, mechanism, and function. Cell 2004;116:281–97.
4. Bartel DP. MicroRNAs: target recognition and regulatory functions. Cell 2009;136:215–33.
5. Friedman RC, Farh KK, Burge CB, Bartel DP. Most mammalian mRNAs are conserved targets of microRNAs. Genome Res 2009;19:92–105.
6. Baffa R, Fassan M, Volinia S, O'Hara B, Liu CG, Palazzo JP, et al. MicroRNA expression profiling of human metastatic cancers identifies cancer gene targets. J Pathol 2009;219:214–21.
7. Iorio MV, Visone R, Di Leva G, Donati V, Petrocca F, Casalini P, et al. MicroRNA signatures in human ovarian cancer. Cancer Res 2007;67:8699–707.
8. Lowery AJ, Miller N, Devaney A, McNeill RE, Davoren PA, Lemetre C, et al. MicroRNA signatures predict oestrogen receptor, progesterone receptor and HER2/neu receptor status in breast cancer. Breast Cancer Res 2009;11:R27.
9. Ryan BM, Robles AI, Harris CC. Genetic variation in microRNA networks: the implications for cancer research. Nat Rev Cancer 2010;10:389–402.
10. Volinia S, Calin GA, Liu CG, Ambs S, Cimmino A, Petrocca F, et al. A microRNA expression signature of human solid tumors defines cancer gene targets. Proc Natl Acad Sci U S A 2006;103:2257–61.
11. Ma L, Teruya-Feldstein J, Weinberg RA. Tumour invasion and metastasis initiated by microRNA-10b in breast cancer. Nature 2007;449:682–8.
12. Medina PP, Nolde M, Slack FJ. OncomiR addiction in an *in vivo* model of microRNA-21-induced pre-B-cell lymphoma. Nature 2010;467:86–90.
13. Voorhoeve PM, le Sage C, Schrier M, Gillis AJ, Stoop H, Nagel R, et al. A genetic screen implicates miRNA-372 and miRNA-373 as oncogenes in testicular germ cell tumors. Advances Experimental Med Biol 2007;604:17–46.
14. Melo SA, Esteller M. Dysregulation of microRNAs in cancer: playing with fire. FEBS Lett 2010;585:2087–99.
15. Chai G, Liu N, Ma J, Li H, Oblinger JL, Prahalad AK, et al. MicroRNA-10b regulates tumorigenesis in neurofibromatosis type 1. Cancer Sci 2010;101:1997–2004.
16. Gabriely G, Yi M, Narayan RS, Niers JM, Wurdinger T, Imitola J, et al. Human glioma growth is controlled by microRNA-10b. Cancer Res 2011;71:3563–72.
17. Moriarty CH, Pursell B, Mercurio AM. miR-10b targets Tiam1: implications for Rac activation and carcinoma migration. J Biol Chem 2010;285:20541–6.
18. Tian Y, Luo A, Cai Y, Su Q, Ding F, Chen H, et al. MicroRNA-10b promotes migration and invasion through KLF4 in human esophageal cancer cell lines. J Biol Chem 2010;285:7986–94.
19. Mestdagh P, Lefever S, Pattyn F, Ridzon D, Fredlund E, Fieuw A, et al. The microRNA body map: dissecting microRNA function through integrative genomics. Nucleic Acids Res 2011;39:e136.
20. Iorio MV, Ferracin M, Liu CG, Veronese A, Spizzo R, Sabbioni S, et al. MicroRNA gene expression deregulation in human breast cancer. Cancer Res 2005;65:7065–70.
21. Schreiber RD, Old LJ, Smyth MJ. Cancer immunoediting: integrating immunity's roles in cancer suppression and promotion. Science 2011;331:1565–70.
22. Herberman RB, Nunn ME, Lavrin DH. Natural cytotoxic reactivity of mouse lymphoid cells against syngeneic acid allogeneic tumors. I. Distribution of reactivity and specificity. Int J Cancer 1975;16:216–29.
23. Kiessling R, Klein E, Wigzell H. "Natural" killer cells in the mouse. I. Cytotoxic cells with specificity for mouse Moloney leukemia cells. Specificity and distribution according to genotype. Eur J Immunol 1975;5:112–7.
24. Guerra N, Tan YX, Joncker NT, Choy A, Gallardo F, Xiong N, et al. NKG2D-deficient mice are defective in tumor surveillance in models of spontaneous malignancy. Immunity 2008;28:571–80.
25. Arnon TI, Markel G, Mandelboim O. Tumor and viral recognition by natural killer cells receptors. Seminars Cancer Biol 2006;16:348–58.
26. Diefenbach A, Raulet DH. Natural killer cells: stress out, turn on, tune in. Curr Biol 1999;9:R851–3.
27. Moretta A, Bottino C, Vitale M, Pende D, Cantoni C, Mingari MC, et al. Activating receptors and coreceptors involved in human natural killer cell-mediated cytolysis. Annu Rev Immunol 2001;19:197–223.
28. Ljunggren HG. Cancer immunosurveillance: NKG2D breaks cover. Immunity 2008;28:492–4.
29. Kim JY, Bae JH, Lee SH, Lee EY, Chung BS, Kim SH, et al. Induction of NKG2D ligands and subsequent enhancement of NK cell-mediated lysis of cancer cells by arsenic trioxide. J Immunother 2008;31:475–86.
30. Nausch N, Cerwenka A. NKG2D ligands in tumor immunity. Oncogene 2008;27:5944–58.
31. Bauman Y, Nachmani D, Vitenshtein A, Tsukerman P, Drayman N, Stern-Ginossar N, et al. An identical miRNA of the human JC and BK polyoma viruses targets the stress-induced ligand ULBP3 to escape immune elimination. Cell Host Microbe 2011;9:93–102.
32. Nachmani D, Lankry D, Wolf DG, Mandelboim O. The human cytomegalovirus microRNA miR-UL112 acts synergistically with a cellular microRNA to escape immune elimination. Nat Immunol 2010;11:806–13.
33. Nachmani D, Stern-Ginossar N, Sarid R, Mandelboim O. Diverse herpesvirus microRNAs target the stress-induced immune ligand MICB to escape recognition by natural killer cells. Cell Host Microbe 2009;5:376–85.
34. Stern-Ginossar N, Elefant N, Zimmermann A, Wolf DG, Saleh N, Biton M, et al. Host immune system gene targeting by a viral miRNA. Science 2007;317:376–81.
35. Stern-Ginossar N, Gur C, Biton M, Horwitz E, Elboim M, Stanietsky N, et al. Human microRNAs regulate stress-induced immune responses mediated by the receptor NKG2D. Nat Immunol 2008;9:1065–73.
36. Thomas M, Lieberman J, Lal A. Desperately seeking microRNA targets. Nat Struct Mol Biol 2010;17:1169–74.

37. van de Wetering M, Oving I, Muncan V, Pon Fong MT, Brantjes H, van Leenen D, et al. Specific inhibition of gene expression using a stably integrated, inducible small-interfering-RNA vector. EMBO Rep 2003; 4:609–15.
38. Xu K, Ma H, McCown TJ, Verma IM, Kafri T. Generation of a stable cell line producing high-titer self-inactivating lentiviral vectors. Mol Ther 2001;3:97–104.
39. Mandelboim O, Reyburn HT, Vales-Gomez M, Pazmany L, Colonna M, Borsellino G, et al. Protection from lysis by natural killer cells of group 1 and 2 specificity is mediated by residue 80 in human histocompatibility leukocyte antigen C alleles and also occurs with empty major histocompatibility complex molecules. J Exp Med 1996;184:913–22.
40. Halfteck GG, Elboim M, Gur C, Achdout H, Ghadially H, Mandelboim O. Enhanced *in vivo* growth of lymphoma tumors in the absence of the NK-activating receptor NKp46/NCR1. J Immunol 2009;182: 2221–30.
41. Lewis BP, Burge CB, Bartel DP. Conserved seed pairing, often flanked by adenosines, indicates that thousands of human genes are microRNA targets. Cell 2005;120:15–20.
42. Ebert MS, Neilson JR, Sharp PA. MicroRNA sponges: competitive inhibitors of small RNAs in mammalian cells. Nat Methods 2007;4: 721–6.
43. Lenac T, Arapovic J, Traven L, Krmpotic A, Jonjic S. Murine cytomegalovirus regulation of NKG2D ligands. Med Microbiol Immunol 2008; 197:159–66.
44. Lanier LL. Up on the tightrope: natural killer cell activation and inhibition. Nat Immunol 2008;9:495–502.
45. Smyth MJ, Swann J, Kelly JM, Cretney E, Yokoyama WM, Diefenbach A, et al. NKG2D recognition and perforin effector function mediate effective cytokine immunotherapy of cancer. J Exp Med 2004;200: 1325–35.
46. Fassati A, Mitchison NA. Testing the theory of immune selection in cancers that break the rules of transplantation. Cancer Immunol Immunother 2010;59:643–51.
47. Elboim M, Gazit R, Gur C, Ghadially H, Betser-Cohen G, Mandelboim O. Tumor immunoediting by NKp46. J Immunol 2011;184:5637–44.
48. Li Y, Wang Q, Mariuzza RA. Structure of the human activating natural cytotoxicity receptor NKp30 bound to its tumor cell ligand B7-H6. J Exp Med 2011;208:703–14.
49. Ma L. Role of miR-10b in breast cancer metastasis. Breast Cancer Res 2010;12:210.
50. Groh V, Rhinehart R, Randolph-Habecker J, Topp MS, Riddell SR, Spies T. Costimulation of CD8alphabeta T cells by NKG2D via engagement by MIC induced on virus-infected cells. Nat Immunol 2001;2: 255–60.